JOURNAL OF SOLID STATE CHEMISTRY **125,** 133–139 (1996)
ARTICLE NO. 0275

Modulated Structure of $La_2NiO_{4+\delta}$ as a Mechanism of Oxygen Excess Accommodation

M. J. Sayagués,*,[1] M. Vallet-Regí,† J. L. Hutchison,* and J. M. González-Calbet‡

*Department of Materials, University of Oxford, Parks Road, Oxford OX1 3PH, United Kingdom; †Departamento de Química Inorgánica y Bioinorgánica, Facultad de Farmacia, Universidad Complutense, 28040-Madrid, Spain; and ‡Departamento de Química Inorgánica, Facultad de Químicas, Universidad Complutense, 28040-Madrid, Spain

Received July 31, 1995; in revised form May 1, 1996; accepted May 8, 1996

A microstructural characterization by means of high resolution transmission electron microscopy has been performed in $La_2NiO_{4+\delta}$ in order to confirm the distribution of the oxygen excess. A structure commensurately modulated along [010] with modulation period $a_S = 3a$, and another with $b_S = 4b$ along [100] were found. The origin of such modulations is discussed in terms of the irregular distribution of interstitial oxygen atoms within the crystal lattice. Although the structural changes may be electron beam induced and these new phases are minorities and possibly metastable, the results contribute new information about how the interstitial oxygen can be accommodated.

INTRODUCTION

$La_2NiO_{4+\delta}$ oxide belongs to the K_2NiF_4 structural type, which is isostructural with $La_2CuO_{4+\delta}$ where high T_c superconductivity was first discovered in 1986 (1). Since then, a considerable amount of work has indicated that superconductivity in this system is related directly to oxygen content. $La_2NiO_{4+\delta}$ exhibits a wide range of oxygen stoichiometry which has been attributed to the presence of intergrown phases or deviation in the metal-atom ratio (2).

The structural changes introduced by the oxygen excess have been widely studied by neutron diffraction and X-ray diffraction techniques in both $La_2NiO_{4+\delta}$ (3, 5) and $La_2CuO_{4+\delta}$ (6, 7) oxides, showing that the oxygen excess is incorporated as an interstitial oxygen defect (O_I), leading to an orthorhombic *Fmmm* structure (3), the (O_I) occupying the (1/4, 1/4, 1/4) sites of such a cell.

In an earlier publication (8) we presented an electron diffraction study of $La_2NiO_{4+\delta}$, which apparently contradicted results obtained by other authors (9–12). However no high resolution transmission electron microscopy (HRTEM) study has been performed, probably due to the fact that the oxygen interstitial can be reduced under the high vacuum conditions required to carry out the experiment.

The correlation between the structure and the microstructure of materials and their physical properties is a point of vital interest in solid state chemistry and HRTEM has played an important role in studying crystals, microstructure, defects, and modulated structures in various types of inorganic oxides. In this paper, we present such a study of $La_2NiO_{4+\delta}$.

EXPERIMENTAL

$La_2NiO_{4+\delta}$ oxide was synthesized from stoichiometric amounts of La_2O_3 and NiO. The mixed powder was heated in air at 1250°C with intermediate grindings. The absolute oxygen content was determined by reducing the sample under pure H_2 at 700°C by means of TGA developed on the basis of a Cahn D-200 electrobalance, with a vacuum and a gas blending system. The oxygen composition obtained was $La_2NiO_{4.14}$. The La : Ni ratio (2 : 1) was confirmed by emission spectroscopy using the Inductive Coupling Plasma method (ICP).

The HRTEM study was performed with a JEOL JEM 4000 EX (II) electron microscope operating at 400 kV and equipped with a top entry ±20° tilt specimen holder.

RESULTS AND DISCUSSION

The powder X-ray diffraction pattern shows a monophasic material which can be indexed on the basis of the K_2NiF_4 tetragonal unit cell.

In order to directly observe the microstructure of the specimen, crystals were carefully selected and oriented into the $[100]_o$, $[010]_o$, and $[\bar{1}10]_o$ directions in the microscope (subindex o refers to the orthorhombic cell proposed by Jorgensen *et al.* (3)). Such a small orthorhombic distortion,

[1] To whom correspondence should be addressed. Permanent address: Departamento de Química Inorgánica, Facultad de Químicas, Universidad Complutense, 28040-Madrid, Spain.

0022-4596/96 $18.00

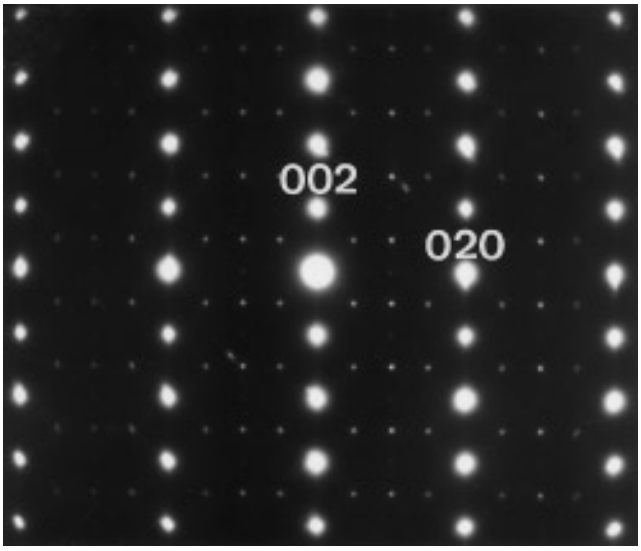

FIG. 1. SAEDP along the $[100]_o$ zone axis for the $La_2NiO_{4.14}$ material.

not observed by X-ray diffraction, was detected by neutron diffraction (3).

Selected area electron diffraction pattern (SAEDP) and HRTEM images of some crystals were recorded.

(*1*) $[100]_o$ *zone axis*. In the majority of the crystals only reflections of the basic structure due to the face-centered orthorhombic (*Fmmm*) unit cell can be seen. However, some crystals show the SAEDP presented in Fig. 1. A fourfold superlattice seems to appear following $(024)^*_o$ and equivalent reflections. The intensity of the first harmonic is larger, suggesting a commensurate modulated structure with $\mathbf{b_S} = 2b$. In the corresponding HRTEM image (Fig. 2a) two different areas of contrast can be observed (marked A and B). Since energy dispersive spectroscopy data suggest that the La–Ni ratio is constant throughout the crystal, the difference in the contrast seems to indicate that the oxygen content is not homogeneously distributed.

Crystallographic image processing (13) was used to check that the extra reflections in the SAEDP (Fig. 1) come only from area A. The results of the Fourier transform of the scanned image in areas A and B are shown in Figs. 3a and 3b, respectively. It is clear that only area A produces superlattice maxima.

Area A (enlarged in Fig. 2b) is very similar in appearance to that found by Yanagisawa *et al.* (14) in the $(Bi_{1-x}Pb_x)_2Sr_2Cu_2O_y$ ($x = 0.2$) compound. The extra oxygen model has been most widely accepted in the bismuth-based superconductors as the origin of structural modulations (15–17). According to this model, this extra oxygen is located between two adjacent (BiO) planes.

On the basis of this information, it can also be proposed that the oxygen excess is responsible for the modulation along the **b** direction in $La_2NiO_{4+\delta}$ and that the interstitial oxygen atoms are located according to neutron diffraction data (3) between two LaO layers. However, in area A it seems that the modulated period is $\mathbf{b_S} = 4b$ instead of $2b$ as suggested by the SAEDP, which means that the space group of the new structure keeps the reflection conditions along the *b* axis (as in *Fmmm* space group). On the other hand, to know exactly which is the oxygen composition in the new structure is difficult. We suggest that, if the new cell has 16 $La_2NiO_{4.+\delta}$ formulas per unit cell ($V_{\text{new cell}} = 4V_{\text{subcell}}$), the δ value could be 0.25 and therefore 4 O_I occupy the unit cell as schematically represented in Fig. 4. The volume of the new cell is 4 times the orthorhombic subcell proposed by Jorgensen *et al.* (3), where the O_I occupy 1/4, 1/4, 1/4 sites. It is worth mentioning that if every subcell (3) was occupied with one O_I, the δ value would be 0.25.

The image contrast was interpreted with the help of the "EMS" image simulation program, using the multislice method (18). In area A, *Pnn*2 seems to be the best space group producing simulated images very similar to the experimental results and the best conditions for the simulation were found for thickness $\tau = 5.4$ nm and defocus $\Delta f = -50$ nm, shown in the inset of Fig. 2b. However, to index all the maxima in the electron diffraction pattern (Fig. 1) the new **c** parameter must be $2\mathbf{c}_o$, probably due to a small distortion in the octahedra (although we cannot detect it in the HREM image). The relationship between the super- and substructure maxima is $(0\,0\,2)^*_o//(0\,0\,4)^*_n$; $(0\,2\,0)^*_o//(0\,8\,0)^*_n$; $(0\,2\,4)^*_o//(0\,8\,8)^*_n$; $(0\,1/2\,1)^*_o//(0\,2\,2)^*_n$; $(0\,1\,2)^*_o//(0\,4\,4)^*_n$; $(0\,3/2\,3)^*_o//(0\,6\,6)^*_n$; $(0\,1\,1)^*_o//(0\,4\,2)^*_n$: subindex n refers to the new orthorhombic cell.

It is worth noting that as a consequence of the heterogeneous distribution of interstitial oxygen, some areas (marked B in Fig. 2a and magnified in Fig. 2c) appear as an ordered phase without a remarkable amount of oxygen excess. The inset corresponds to a simulated image, which was performed under the conditions of thickness $\tau = 8$ nm and defocus $\Delta f = -50$ nm. The existence of crystals with δ values between 0 and 0.25 would justify the δ average value (0.14) found by mean of thermogravimetric measurements.

(*2*) $[010]_o$ *zone axis*. Figure 5a shows the SAEDP along the $[010]_o$ zone axis, where satellite reflections due to a modulated structure along the $\mathbf{a}^*_o$ direction can be seen. There are five rows of weaker maxima between the $(00l)^*_o$ and $(20l)^*_o$ basic reflections, suggesting that the modulated structure is commensurate with $\mathbf{a_S} = 3a$. This kind of modulation has been found in most of the crystals along such a zone axis. The corresponding micrograph is presented in Fig. 5b.

On the other hand this SAEDP can be described as a sixfold superlattice along [203]* and a twofold superlattice

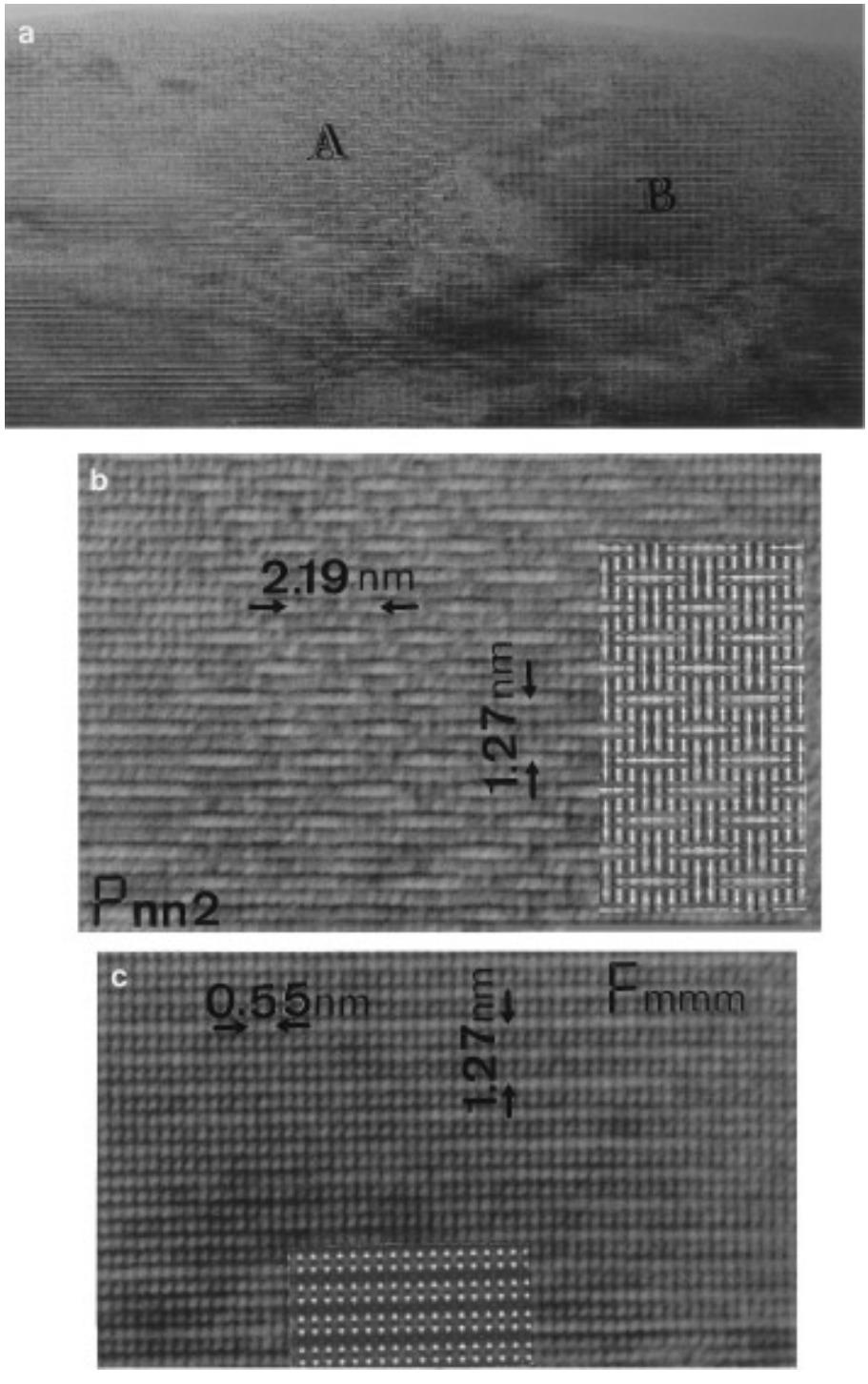

FIG. 2. (a) HRTEM micrograph along the $[100]_o$ zone axis for the $La_2NiO_{4.14}$ material. (b) Area A enlarged; the inset shows a calculated image for the modulated structure along the $[100]_o$ zone axis. (c) Area B enlarged; the inset shows a calculated image for the basic subcell along the $[100]_o$ zone axis.

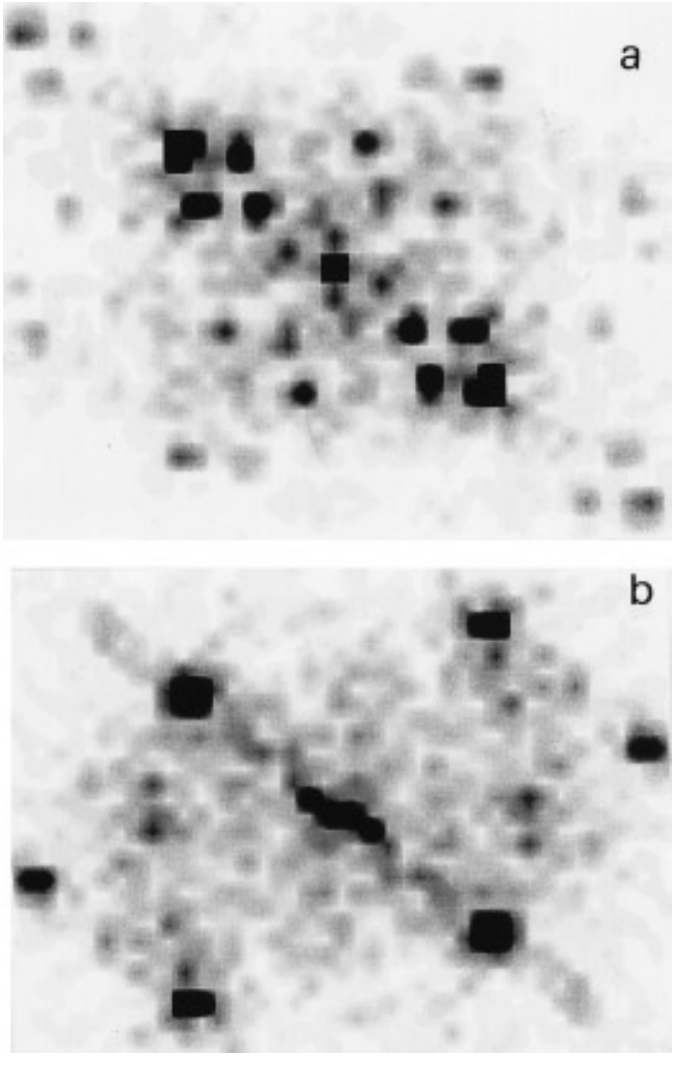

FIG. 3. Fourier transform of the scanned image shown in Fig. 2a (a) for area A and (b) for area B.

along [001]*. According to these superstructure directions, a matrix relationship between the orthorhombic (*Fmmm*) and the new structure (in the reciprocal and real space) can be established:

$$\begin{pmatrix}\mathbf{a}\\ \mathbf{b}\\ \mathbf{c}\end{pmatrix}^* = \begin{pmatrix}2/6 & 0 & 3/6\\ 0 & 1 & 0\\ 0 & 0 & 1/2\end{pmatrix} \times \begin{pmatrix}a_0\\ b_0\\ c_0\end{pmatrix}^*$$

$$\begin{pmatrix}\mathbf{a}\\ \mathbf{b}\\ \mathbf{c}\end{pmatrix} = \begin{pmatrix}\bar{3} & 0 & 0\\ 0 & 1 & 0\\ 3 & 0 & 2\end{pmatrix} \times \begin{pmatrix}a_0\\ b_0\\ c_0\end{pmatrix}.$$

The new cell has monoclinic symmetry with parameters

$$\mathbf{a} = 3a_o = 1.632 \text{ nm}$$
$$\mathbf{b} = b_o = 0.547 \text{ nm}$$
$$\mathbf{c} = -3a_o + 2c_o = 3.021 \text{ nm}.$$

In this structure the modulation period is smaller than in the previous one. The monoclinic distortion is produced due to the wave of modulation being slightly shifted along the **a** axis from one LaO layer to another. The composition could be $La_2NiO_{4.25}$ ($V_{\text{new cell}} = 6V_{\text{subcell}}$), leading to 6 O_I per unit cell as shown schematically in Fig. 6.

The *P*2/*m* space group was used to simulate the experimental image, the best image match being found under conditions of thickness $\tau = 14.5$ nm and defocus $\Delta f = -50$ nm, shown in the inset of Fig. 5c.

(*3*) $[\bar{1}10]_o$ *zone axis.* The SAEDP along the $[\bar{1}10]_o$ zone axis is shown in Fig. 7a, where very weak superlattice

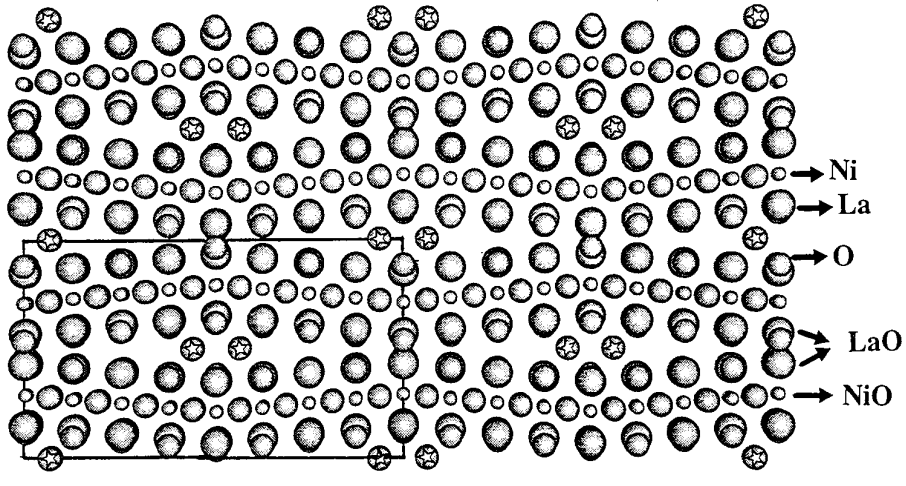

FIG. 4. Hypothetical crystal structure of $La_2NiO_{4.25}$ (S-I) projected along the **a** direction. A unit cell of the commensurate modulated structure with $b_S = 4b$ is shown with a rectangle (O_I atoms are indicated by ⊛).

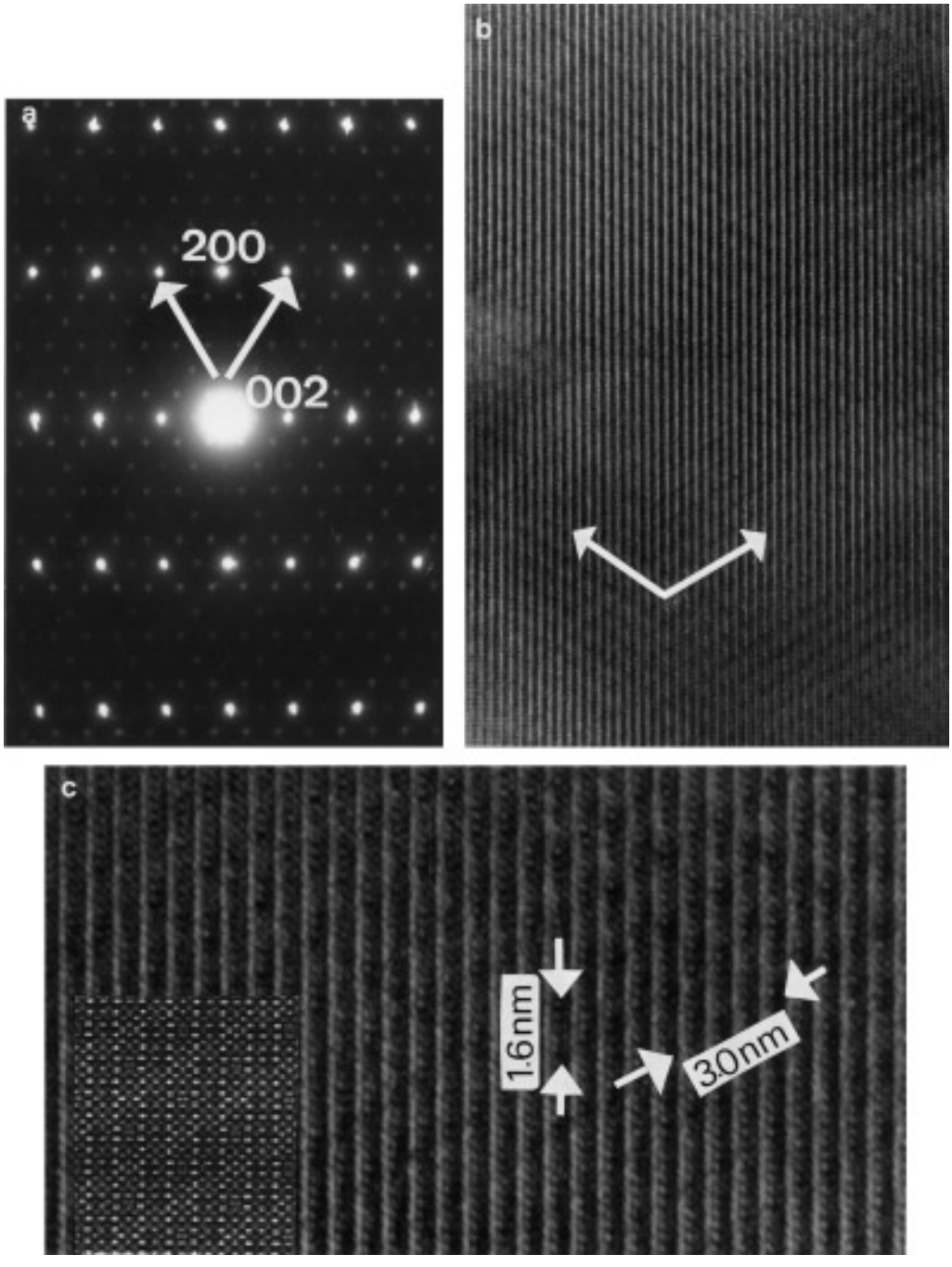

FIG. 5. (a) SAEDP along the $[010]_o$ zone axis for the $La_2NiO_{4.14}$ material. (b) Corresponding micrograph. (c) Enlargement of the previous micrograph; the inset shows a simulated image for the modulated structure along such zone axis.

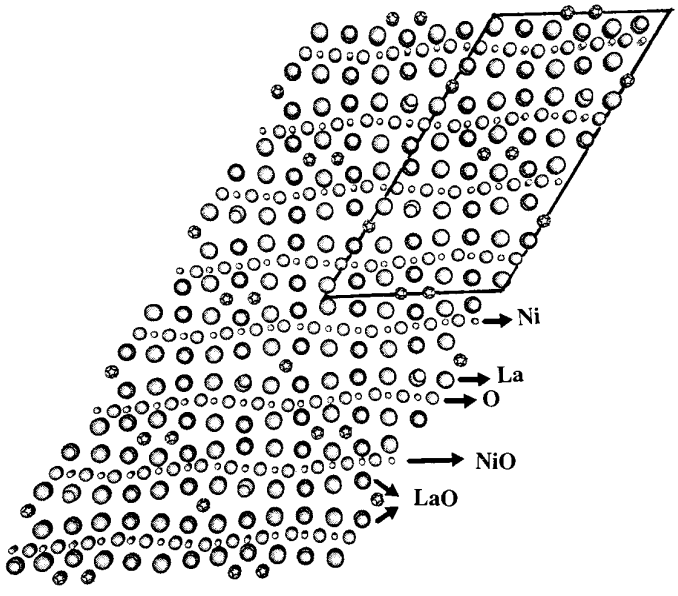

FIG. 6. Hypothetical crystal structure of $La_2NiO_{4.25}$ (S-II) projected along the **b** direction. A unit cell of the commensurate modulated structure with $\mathbf{a_S} = 3a$ is shown (O_I atoms are indicated by ⊛).

maxima along the $[111]_o$ direction can be seen. However, in the corresponding micrograph (Fig. 7b) only the contrast due to the atoms in the normal positions for the *Fmmm* space group can be observed. The inset shows the simulated image more similar to the experimental image (thickness $\tau = 8$ nm and defocus $\Delta f = 55$ nm).

CONCLUSIONS

On the basis of these results, it seems that the O_I in this sample is not homogeneously distributed, the majority of it being located in some areas leading to two different modulated structures (found in different crystals) whose modulation periods are $\mathbf{b_S} = 4b$ (S-I) and $\mathbf{a_S} = 3a$ (S-II). However, both correspond to the $La_2NiO_{4.25}$ formula, thus implying that the same oxygen composition may adopt several distributions of O_I leading to different modulated structures.

It is worth mentioning that the same sample was studied by SAED (6) in a JEOL 2000 FX microscope, where we found that the ordering of the interstitial oxygen led to a new homologous series of the general formula $La_{8n}Ni_{4n}O_{16n+1}$ in which the oxygen excess is ordered along the

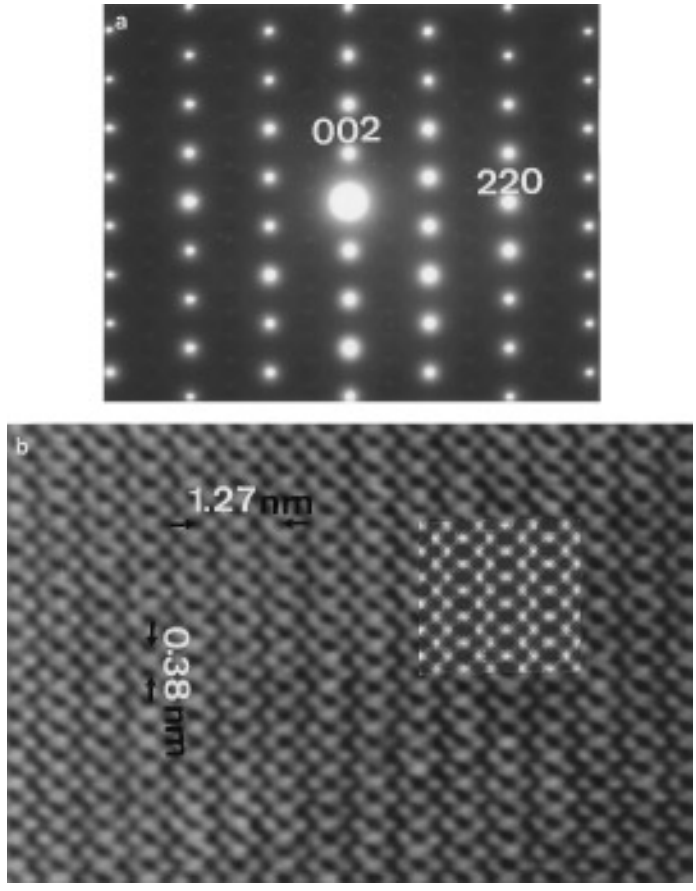

FIG. 7. (a) SAEDP along the $[\bar{1}10]_o$ zone axis for the $La_2NiO_{4.14}$ material. (b) Corresponding micrograph; the inset shows a simulated image for the basic subcell along the $[\bar{1}10]_o$ zone axis.

$[01\bar{1}]_t$ direction (subindex t refers to the K_2NIF_4 tetragonal cell, $I4/mmm$).

However, the present results are somewhat different for the same sample. This suggests that in some crystals the oxygen excess is being removed under the reducing conditions of the experiment, whereas in other crystals, areas richer in oxygen have actually been created by means of radiation under the electron beam, probably due to the liability of the interstitial oxygen.

ACKNOWLEDGMENTS

We thank the ''Ministerio de Educación y Ciencia'' in Spain and the University of Oxford for financial support. J. M. Martínez and S. Nicolopoulos provided valuable assistance with computer programming.

REFERENCES

1. J. G. Bednorz and K. A. Müller, *Z Phys. B* **64,** 189 (1986).
2. D. J. Buttrey, H. R. Harrison, J. M. Honig, and R. R. Schartman, *J. Solid State Chem.* **54,** 407 (1984).
3. J. D. Jorgensen, B. Dabrowski, S. Pei, D. R. Richards, and D. G. Hinks, *Phys. Rev. B* **40,** 2187 (1988).
4. J. Rodríguez, M. T. Fernández, and J. L. Martínez, *J. Phys. Condens. Matter.* 3215 (1991).
5. D. E. Rice and D. J. Buttrey, *J. Solid State Chem.* **105,** 197 (1993).
6. J. D. Jorgensen, B. Dabrowski, S. Pei, D. G. Hinks, L. Soderholm, B. Morosin, J. E. Shirber, E. L. Venturini, and D. S. Ginley, *Phys. Rev. B* **38,** 11337 (1988).
7. C. Chaillout, J. Chenavas, S. W. Cheong, Z. Fisk, M. Marezio, B. Morosin, and J. E. Schirber, *Physica C* **70,** 87 (1990).
8. M. J. Sayagués, A. Caneiro, J. M. González-Calbet, and M. Vallet-Regí, *J. Matter. Res.* **9,** 1263 (1994).
9. Z. Hiroi, T. Obata, M. Takano, and Y. Bando, *Phys. Rev. B* **41,** 11665 (1990).
10. A. Demourgues, F. Weill, J. C. Grenier, A. Wattiaux, and M. Pouchard, *Physica C* **192,** 425 (1992).
11. L. C. Otero-Díaz, A. R. Landa, F. Fernández, R. Sáez-Puche, R. Withers, and B. G. Hyde, *J. Solid State Chem.* **97,** 443 (1992).
12. A. Demourgues, F. Weill, B. Darriet, A. Wattiaux, J. C. Grenier, P. Gravereau, and M. Pouchard, *J. Solid State Chem.* **106,** 317 (1993).
13. D. X. Li and S. Hovmöller, *J. Solid State Chem.* **73,** 5 (1988).
14. K. Yanajisawa, Y. Matsui, K. Shoda, E. Takayama-Muromachi, and S. Horiuchi, *Physica C* **196,** 34 (1992).
15. H. W. Zandbergen, W. A. Groen, F. C. Mijhoff, G. van Tendeloo, and S. Amelinckx, *Physica C* **156,** 325 (1988).
16. M. Takano, J. Takeda, K. Oda, H. Kitaguchi, Y. Miura, Y. Ikeda Y. Tomii, and H. Mazaki, *Jpn. J. Appl. Phys.* **27,** L1041 (1988).
17. A. Yamamoto, M. Onoda, E. Takayama-Muromachi, F. Izumi, T. Ishigaki, and H. Asano, *Phys. Rev. B* **42,** 4228 (1990).
18. P. A. Stadelmann, ''EMS Program'' 12M-EPFL, CH-1015 Lausanne, Switzerland, 1993.